THIS MONTH IN

JNM

PET in cancer immunotherapy: Tumeh and colleagues review current molecular imaging approaches for differentiating metabolically active cancer cells from activated immune cells. . . . . ***Page 865***

Cellular uptake of radioactivity: Bolch reviews recent developments in cellular uptake models of radiopharmaceuticals and previews an article on this topic in this issue of *JNM*. . . . . ***Page 869***

Peripheral uptake reproducibility: Rudd and colleagues compare the accuracy of 2 methods of measuring short-term ^{18}F-FDG uptake in PET imaging to assess therapies in peripheral artery disease. . . ***Page 871***

Phase 1 ^{18}F-AH111585 trial: Kenny and colleagues investigate the safety, stability, and tumor distribution kinetics of this novel RGD-based integrin peptide–polymer conjugate and its suitability for use with PET to detect tumors in patients with metastatic breast cancer. . . . . ***Page 879***

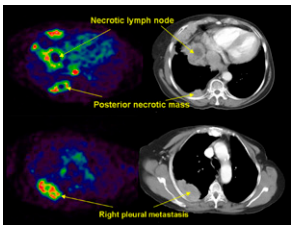

Enhanced metabolism after tumor removal: Scheer and colleagues use ^{18}F-FDG PET to evaluate the metabolic activity of liver metastases before and after resection of primary colorectal tumors and discuss the implications for administration of postoperative antiangiogenic therapy. . . . . ***Page 887***

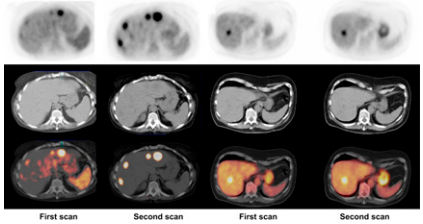

Tumor volumes from metabolic rate maps: Visser and colleagues determine tumor volumes in glucose metabolic rate maps, compare these with standardized uptake value maps, and describe the benefits of additional metabolic information in PET-based radiotherapy planning and response monitoring. . . . ***Page 892***

^{99m}Tc-EC20 tumor imaging: Fisher and colleagues measure accumulation percentages of this novel folate receptor–targeted imaging agent in patients with various solid tumors and correlate uptake with immunohistochemistry analyses of receptor expression in biopsied tumor tissue. . . .***Page 899***

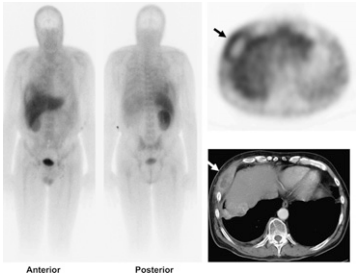

^{123}I-MIBG in CHF: Kasama and colleagues explore whether serial ^{123}I-MIBG scintigraphic studies represent a reliable prognostic marker for death and sudden death in patients with congestive heart failure. . . . . ***Page 907***

SPECT attenuation correction in women: Wolak and colleagues assess the performance of attenuation correction in women, using automated quantitative analyses in myocardial perfusion SPECT to avoid bias. . . . . ***Page 915***

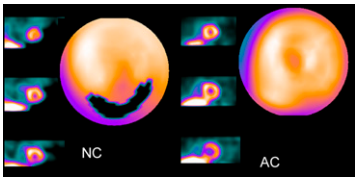

Radioiodine and ophthalmopathy: Sisson and colleagues report on rates of appearance or increase in manifestation of Graves ophthalmopathy in U.S. patients treated with radioiodine for hyperthyroidism. . . . . ***Page 923***

PET in focal epilepsy: O'Brien and colleagues apply decision tree analysis to evaluate the sensitivity, specificity, and cost effectiveness of clinical algorithms that incorporate ^{18}F-FDG PET in the presurgical assessment of medically refractory focal epilepsy. . . . . ***Page 931***

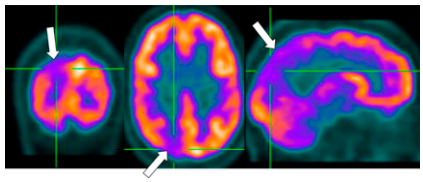

Dual-modality imaging: Townsend provides an educational overview and perspectives on the development of image fusion techniques and looks at advances and challenges in using image fusion from complementary modalities to provide more complete and accurate assessments of disease. . . . . ***Page 938***

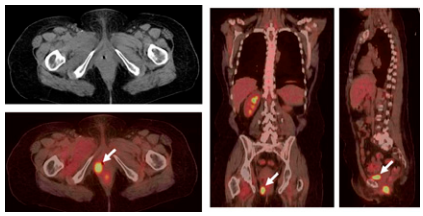

Camera for sentinel node biopsy: Tsuchimochi and colleagues report on animal studies evaluating the efficacy of a small cadmium telluride γ-camera intended for use in radioguided surgeries. . . .***Page 956***

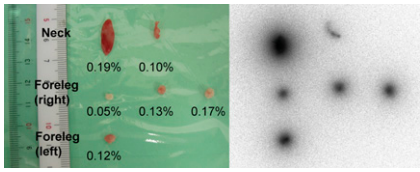

Quantitation of CXCR4 expression: Misra and colleagues describe in vivo quantification of this chemokine stromal-derived factor-1α and its receptor and discuss the potential for elucidating mechanisms of cardiac dysfunction in a variety of animal models of disease. . . ***Page 963***

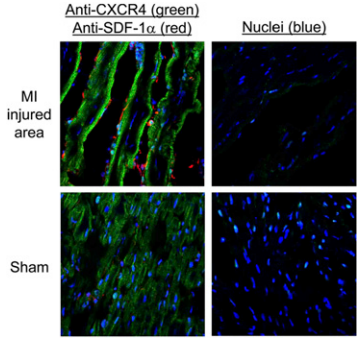

^{99m}Tc-lisinopril for ACE imaging: Femia and colleagues detail the synthesis and evaluation of lisinopril probes for imaging angiotensin-converting enzyme expression and highlight the promise for monitoring enzyme expression as a function of cardiac disease progression. . . . . ***Page 970***

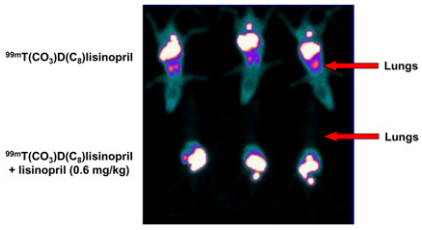

Estradiol-based imaging agent: Nayak and colleagues report on synthesis, biodistribution, and nanoSPECT/CT studies in a new structural class of compounds for potential use in breast and endometrial cancer imaging. . . . . ***Page 978***

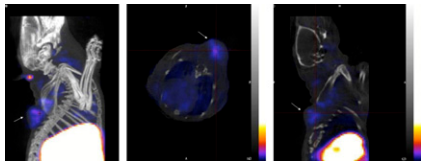

^{18}F-labeled androgen ligands: Parent and colleagues evaluate 2 novel ^{18}F-labeled androgens with potential for use in clinical imaging trials to explore the role of sex hormone–binding globulin in radiotracer delivery of steroidal systems to targeted tissues. . . . . ***Page 987***

Ubiquicidin PET tracers in abscesses: Salber and colleagues compare the distribution of ^{18}F- and ^{99m}Tc-labeled ubiquitin compounds in PET imaging of muscle abscesses with the results of anti-*Staphylococcus aureus* immunofluorescent imaging. . . . . ***Page 995***

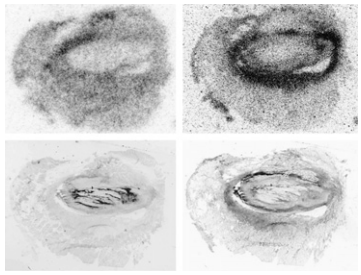

Resolution modeling in PET: Sureau and colleagues assess the impact of resolution modeling during reconstruction on image quality and on estimates of biologic parameters in clinical and phantom brain studies on a high-resolution research tomograph. . . . . ***Page 1000***

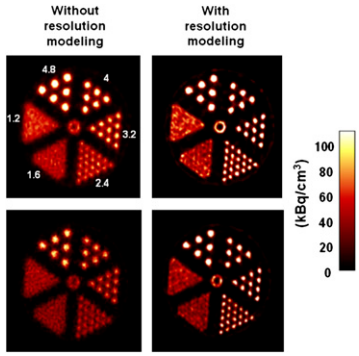

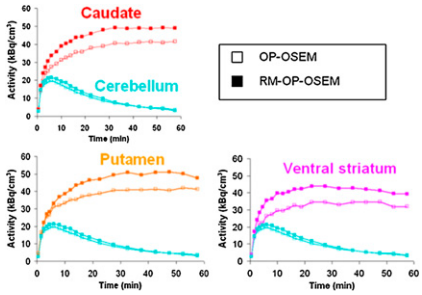

Statistical analysis of α-particle tracks: Neti and Howell report on a detailed analysis of earlier autoradiographic data on distribution of radioactivity among a population of cells labeled with ^{210}Po. . . . . ***Page 1009***

^{124}I PET dosimetry protocol for DTC: Jentzen and colleagues research the iodine kinetics and lesion dose per administered ^{131}I activity of differentiated thyroid cancer metastases using ^{124}I PET to derive an optimized dosimetry protocol. . . . ***Page 1017***

Pediatric radiopharmaceutical dosimetry: Treves and colleagues report on the results of a survey of North American pediatric hospitals to determine the range of variability in radiopharmaceutical dosimetry and the implications for variability in radiation-absorbed doses. . . . ***Page 1024***

ON THE COVER

Atherosclerosis imaging with ^{18}F-FDG PET is useful for detecting inflammation within plaque and monitoring the response to drug therapy. Here, PET and PET/CT images of femoral artery ^{18}F-FDG uptake on days 1 and 14 demonstrate the strong temporal reproducibility of the technique. Measurement of target-to-background ratios may prove useful for assessing both systemic and plaque-focused therapies for atherosclerosis.

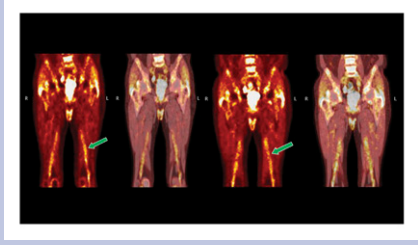

See page 873.